An Improved Hierarchy Ranking Method with Adaptive Weighted Coefficient for Multimodal Multiobjective Optimization

Hejun Xuan, Yan Ding, Lei Xie, Junyi Hu, Yuhang Niu, and Yan Feng

***Abstract*—Multimodal multiobjective problem (MMOPs) is a class of multiobjective optimization problems where multiple Pareto Sets (PSs) in the decision space corresponding to the same Pareto Front (PF) in the objective space, and they are widely prevalent in real-life applications. However, a more realistic situation in engineering problems is when the objective value of one solution is a little worse than another and these solutions are far from one another in the decision space. Furthermore, when dealing with MMOPs, it is common to search for both global and local PSs. In addition, most state-of-the-art multimodal multiobjective evolutionary algorithms (MMEAs) have a poorly convergence and cannot always acquire all PSs. To tackle these problems, this study proposed an improved hierarchy ranking method with adaptive weighted coefficient for MMOPs, called HREA-AWC. Firstly, an adaptive weighting coefficient method is proposed to avoided falling into a local optimum and can improved the global convergence ability. Secondly, crowding distance estimation strategy based on the 2-norm, which helped the algorithm identify and maintain multiple PSs, is designed. Thirdly, a dual offspring generation strategy, which can promote the diversity of the algorithm in the objective space and decision space, is presented. Finally, large number of experiments have been conducted, and the experimental results showed that HREA-AWC has a better performance than compared algorithms for solving the benchmark problems.**

***Index Terms*—multimodal multiobjective, evolutionary computation, adaptive weighed coefficients, crowding distance estimation.**

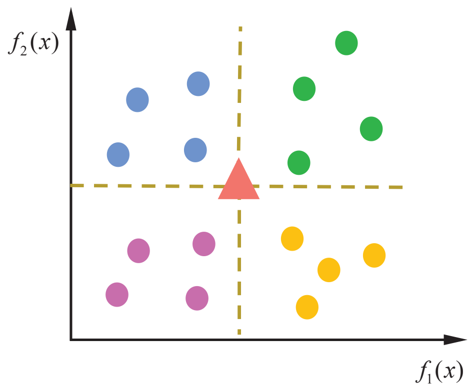

Fig. 1: Relation of dominance.

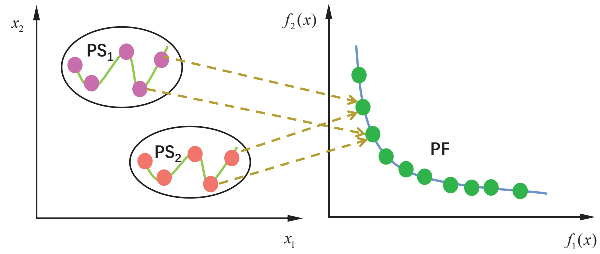

Fig. 2: Multimodal multiobjective optimization.

I. Introduction

MULTIOBJECTIVE Optimization Problems (MOPs) are special optimization problems that need to consider multiple objective functions at the same time[1]. Unlike traditional single-objective optimization problems, there is usually no one solution that can meet all objectives at the same time. Therefore, coordination and compromise between different objectives exits. The goal of multiobjective optimization problem is to find a set of solutions that provide the best trade-off between different objectives. The set of solutions is called the Pareto Set (PS). In general, MOPs can be formulated as follows:

$$\begin{cases} \min F(x) = \{f_1(x), f_2(x), \dots, f_m(x)\} \\ s.t. \\ \quad x = (x_1, x_2, \dots, x_n) \in \Omega \end{cases} \tag{1}$$

where $F(x)$ represents m objective functions, and x is a vector of decision variables. Ω denotes the feasible domain of all decision variables x.

The dominate relationship is defined as follows: x_a is dominate x_b iff $\forall i = 1, 2, \dots, m$, $f_i(x_a) \le f_i(x_b)$ and $\exists j = 1, 2, \dots, m$, $f_j(x_a) < f_j(x_b)$, denoted as $x_a \prec x_b$. Moreover, a Pareto optimal solution is that the solution isn't dominated by any other solutions. As shown in Fig. 1, this is a two-objective minimizing problem, in which the optimization direction of $f_1(x)$ is from right to left, and the optimization

Manuscript received December 14, 2024; revised March 23, 2025. This work was supported by National Natural Science Foundation of Henan Province (No.232300420424), Henan Province Key Research and Development Project (No.241111212200), Henan Joint Fund for Science and Technology Research(No.20240012), Science and Technology Department of Henan Province (No.242102211070).

Hejun Xuan is an associate professor at the School of Computer and Information Technology, Xinyang Normal University, Xinyang Henan, 46400, China. (Corresponding author, email: xuanhejun0896@xynu.edu.cn)

Yan Ding is a graduate student at the School of Computer and Information Technology, Xinyang Normal University, Xinyang Henan, 46400, China. (email: 1151812253@qq.com)

Lei Xie is an associate professor at the School of Computer and Information Technology, Xinyang Normal University, Xinyang Henan, 46400, China. (email: xielei237@xynu.edu.cn)

Junyi Hu is a graduate student at the School of Computer and Information Technology, Xinyang Normal University, Xinyang Henan, 46400, China. (email: 2791848355@qq.com)

Yuhang Niu is a graduate student at the School of Computer and Information Technology, Xinyang Normal University, Xinyang Henan, 46400, China. (email: 2391644131@qq.com)

Yan Feng is a professor at the School of Computer and Information Technology, Xinyang Normal University, Xinyang Henan, 46400, China. (email: fengyan_xynu@126.com)

direction of $f_2(x)$ is from top to bottom. Assuming that the circle and the triangle in the Fig. 1 represents different solutions. The purple circles dominate the red triangle. The green circles are dominated by the red triangle. However, the red triangle is not dominated by the blue circles and the yellow circles. As shown left of in Fig. 2, the set consisting of non-dominated solutions in the decision space is called the Pareto Sets (PS). As shown right of Fig. 2. The image of the PS in objective space is known as the Pareto Front(PF).

Many engineering problem can be modeled as a multiobjective model. In addition, multiple different solutions have the same or similar objective values, which is called a multimodal multiobjective problem (MMOPs). As shown right of in Fig. 2. The study of multimodal multiobjective optimization problems (MMOPs) is crucial for providing diverse solutions, offering decision makers multiple high quality options when faced with complex challenges. These problems often have multiple global or local optimas in practical applications such as network optimization [2], path selection [3], production scheduling [4], VNF service chain deployment [5], [6], and protein design [7]. MMOPs can enhance overall understanding of the issues, and can help to avoid difficulties or economic losses. Furthermore, the development of multimodal multiobjective evolutionary algorithms (MMEAs) has advanced both evolutionary algorithms and multiobjective optimization theory, fostering technological innovation and addressing real-world problems. Thus, research on MMOPs holds significant theoretical importance and valuable practical application.

When addressing multimodal multiobjective optimization problem, two major challenges are encountered: (1) How to enhance the search capability of algorithm to discover as many Pareto optimal solutions as possible during the search process. (2) How to effectively preserve solutions that are close in the objective space but distant in the decision space during environmental selection, while ensuring diversity in both the decision and objective spaces. To tackle these two key difficulties, researchers have developed a variety of multiobjective evolutionary algorithm (MOEA), which aims to find a set of solutions in the objective space that not only perform well on individual objectives but also present a good distribution over the entire solution set. In multiobjective optimization, researchers usually focus on two key criteria: convergence and diversity. Convergence refers to the ability of the algorithm to drive the population towards the Pareto Front (PF), while diversity refers to its ability to maintain a broad distribution of the solution set across the objective space. Therefore, advanced MOEA, like NSGA-II [8], MOEA/D [9], BoTAPDTA [10], CTBOA [11] and PICEA [12], perform well in multiobjective optimization benchmarks. These algorithms can efficiently estimate the Pareto front while maintaining the diversity of the solution set through well-designed operators and strategies.

Although some progress has been made in multimodal multiobjective optimization, existing researches mainly focused on the optimization of a single or a few objectives. When dealing with complex problems that have multiple conflicting objectives, it is often difficult for designing algorithms to achieve optimal solutions for all objectives. Traditional multimodal multiobjective evolutionary algorithms tend to solve multiple Pareto solutions with the same objective value. However, it is more practical in engineering problems where one solution is slightly worse than another in terms of objective value and these solutions are far apart in the decision space. In other words, these problems have global and local Pareto fronts. Due to Pareto domination, the population is likely to convergence quickly to the global PSs. Most multimodal multiobjective evolutionary algorithms attempt to abandon the local PS, which may cause the algorithm to fall into a region of local optima. To tackle this problem, a novel MMEA based on hierarchical ranking method called HREA [13] is proposed for obtaining global PSs and local PSs. Specifically, the algorithm proposes the use of local convergence quality to maintain all global PS and local PS in the main population. In the convergence archive, a hierarchy ranking method is used to improve the convergence ability and to control the quality of local PFs. With the hierarchy ranking method, HREA can well balance the diversity and convergence of the resulting solutions. In addition, a local convergence quality evaluation method to better maintain diversity in the decision space.

Inspired by HREA, this study proposed an improved hierarchy ranking method with adaptive weighted coefficient for multimodal multiobjective optimization, called HREA-AWC. The adaptive weighting strategy dynamically adjusts weights coefficient based on the algorithm's current iteration and population distribution. The 2-norm crowding distance strategy makes the Pareto optimal solution as dispersed as possible in the objective space by assigning a crowding distance to each individual, ensuring a uniform distribution of solutions across the Pareto front and helping to find a more comprehensive set of optimal solutions. Specifically, the dual offspring generation strategy produces offspring that can quickly convergence near the optimal solution, especially in the early stages of the algorithm, thereby reducing calculative time and the number of iterations. The HREA-AWC aims to obtain all global and local PSs while enhancing the convergence of MMEAs. In summary, the main contributions of this paper are summarized as follows:

- An adaptive weighting coefficient method, which can avoid falling into a local optimum and improved the global convergence ability, is designed.
- To helped the algorithm identify and maintain multiple PSs, a crowding distance estimation strategy based on the 2-norm is proposed.
- For the sake of promoting the diversity of the algorithm in the objective space and decision space, a dual offspring generation strategy is designed.

The rest of this paper is organized as follows: Section II described the proposed algorithm in detail. Section III and Section IV demonstrates the experimental setting, effectiveness of proposed algorithm with extensive experiments. Conclusions are given in Section V.

II. Proposed Algorithm

A. General Framework of HREA-AWC

Like MOEAs, the framework of HREA-AWC consists of the following parts: population initialization, environmental selection, archives update, and offspring generation. The framework of HREA-AWC is described in Fig. 3. Firstly,

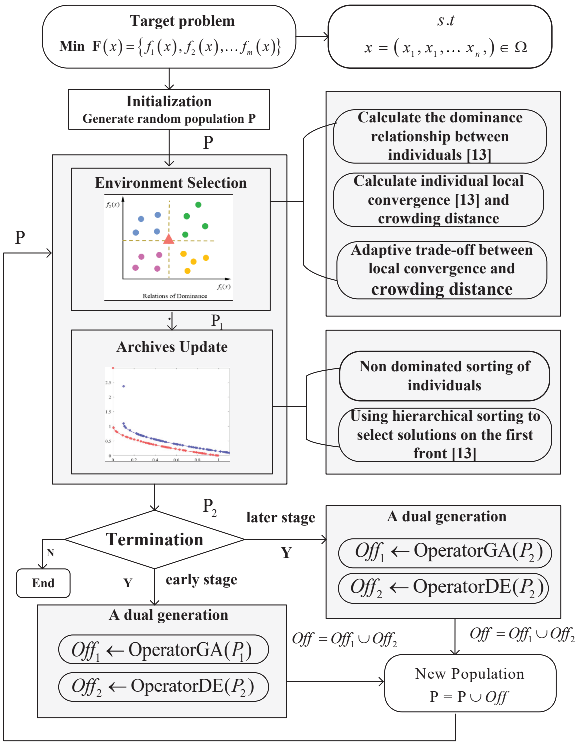

Fig. 3: Framework of HREA-AWC.

initialize N individuals to form a population P. Then, individuals in population P are used to environmental selection and archive updates, resulting in populations P_1 and P_2. Secondly, make judgments based on the conditions. When the conditions are satisfied, the dual offspring (Off_1 and Off_2) is generated and merged into P. Finally, the merged new population P is returned to the environment selection and archive update for the next iteration. When the conditions are not met, the algorithm stopped.

In the process of environmental selection, inspiration is drawn from the ideas of HREA [13]. Firstly, calculate the non-dominated relationships in the population. Secondly, calculate the local convergence and crowding distance. Thirdly, a novel adaptive weight coefficient strategy to dynamically adjust local convergence and crowding distance, which comprehensively evaluate the quality of individuals and select individuals with excellent performance as population P_1.

When updating the archives, like most evolutionary algorithms, non-dominated sorting for the population is adopted. Then, similar to HREA [13], individuals are sorted and the first front is selected. Finally, generate population P_2.

In generating offspring, this paper introduced a dual generation strategy that can enhance the algorithm's ability to discover multiple Pareto solution. There are roughly two stages: In early stage, offspring are selected from the main population using genetic operators with differential evolution operators. In later stage, offspring are randomly chosen from the archive using genetic operators and differential evolution operators. In each generation, different offspring are selected from both the population and the convergence archive. This co-evolutionary approach, while not novel in the context of MOEAs tackling MOPs, is exemplified in algorithms like CCMO [14] and c-DPEA [15] for balancing constraints and exploration efficacy, and in CPDEA [16] and MMEA-WI [17] for maintaining a balance between diversity and convergence.

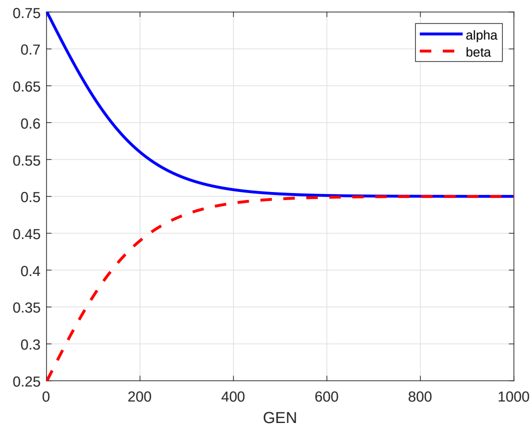

Fig. 4: The curves of α and β.

B. Adaptive Weighting Coefficient Strategy

Algorithm 1: Adaptive weighting coefficient strategy

Input: Pop, population size N, α.
Output: Pop$_1$, crowding distance PopCD.

1 L_C = LocalC (UnionPop) /*Refer to the [13];
2 PopCD $\leftarrow$ sum(dist(1:3,:));
3 NewPop $\leftarrow$ sortrow([$\alpha \cdot L_C$, $\beta \cdot$ PopCD]);
4 PopCD $\leftarrow$ Crowding(NewPop);
5 Return Pop$_1$, PopCD.

Algorithm 1 is the main process of adaptive weighting coefficients. Firstly, calculate the L_c of the population (line 1). At the same time, calculate the crowding distance of the population and select from first to third columns for addition (line 2). Then, using a parameter α, adaptively adjust the weights of L_c and crowding distance to obtain a new population (line 3). Secondly, using a new crowding measurement method constructed with 2-norm and harmonic mean, calculate the crowding distance of the new population again (line 4). Finally, return the distance between the new population and the new crowding distance (line 5). The following method is adopted to adaptively adjust the weights of L_c and crowding distance:

$$\alpha = 1 - (0.5/(1 + e^{M \times \frac{-(gen-1)}{GEN}})) \tag{2}$$

where, the adjustment coefficients for α is based on the current iteration count gen and the maximum iteration count GEN. After extensive experimental verification, the optimal value for M is 10.

The calculation of α utilizes the logistic function, which is a common s-shaped function that typically ranges between -1 and 1, but here it is adjusted to range between 0 and 1. As gen approaches GEN, α gradually decreases. As shown in Fig. 4. The blue line represents α. β is indicated by the red line. β increases with the number of iterations.

$$Mat = \alpha \times L_c + \beta \times Dis \tag{3}$$

A matrix named Mat is a weighted sum of two matrices. L_c is local convergence. Dis represents the diversity of the population, and Dis takes individuals with larger distances. α is used to weight of L_c and β is used to weight of Dis. Among them, β is equal to $(1-\alpha)$. Thereby, Mat combines feature on local convergence and population diversity.

During environmental selection, the population is sorted by using a parameter that integrates local convergence and population diversity. In the initial stage, the weight of local convergence is relatively high, which helps accelerate convergence. As evolution progresses, α gradually decreases and the impact of crowding distance gradually increases, which encourages the population to search for more diverse solutions and avoid falling into local optima. The weighting method enables the optimization process to make adjustments at different stages according to the needs of the problem, balancing the relationship between exploration diversity and convergence. The α dynamically adjusts the weights assigned to these components at different stages of the algorithm. As the algorithm advances, the α evolves, enabling a dynamic adjustment of the sorting strategy.

C. Crowding Distance Estimation Based on the 2-Norm

As shown in Algorithm 1. In this study, we use the 2-norm and harmonic mean methods to estimate the density of solutions in the decision space:

$$Dis = \frac{N-1}{\sqrt[2]{\sum_{j=1}^{N} 1/\|x_j - x_i\|_2}} \tag{4}$$

where N indicates population size. $\| x_j - x_i \|_2$ indicates the Euclidean distance of solutions x_i and x_j. Note that x_i and x_j have been previously normalized. This crowding distance metric is crucial for maintaining diversity and guiding the search process in multiobjective optimization problems.

D. A Dual Offspring Generation Strategy

Algorithm 2 is the main process of dual offspring generation strategy. Initialize the population (line 1). Select the preserved population Pop_1 and crowding distance PopCD through environmental selection (line 2). Update the archive to retain population Pop_2 and congestion ArcCD (line 3). Calculate the fitness of Pop_2 (line 4). Termination condition not met, execute loop. In the early stage of iteration, individuals of crowding distance PopCD will be selected and the selected individuals will be retained in MPool_1 (line 12). The individuals selected by genetic algorithm in MPool_1 are retained in Offspring_1 (line 13). Next, individuals of fitness will be selected and the selected individuals will be kept in MPool_2 (line 14). The individuals selected by differential evolution algorithm in MPool_1 are retained in Offspring_2 (line 15). In the later stage of iteration, individuals of ArcCD will be selected and the selected individuals will be retained in MPool_1 (line 7). The individuals selected by genetic algorithm in MPool_1 are retained in Offspring_1 (line 8). Next, individuals of fitness will be selected and the selected individuals will be kept in MPool_2 (line 9). The individuals selected by differential evolution algorithm in Mpool_2 are retained in Offspring_2 (line 10). Finally, merge the Offspring_1 and Offspring_2 obtained in the early and later stages (line 17). Merge Pop and Offspring to obtain a new population UnionPop (line 18).

Algorithm 2: A dual offspring generation strategy.

```
   Input: Pop, population size N.
   Output: UnionPop (Pop ⋃ Off_1 ⋃ Off_2).
1  Pop ← Initialization (N);
2  [Pop_1, PopCD] ← EnvSel (Pop, N);
3  [Pop_2, ArcCD] ← ArcUpdata (Pop, N);
4  Fitness ← CalFitness (Pop_2, N);
5  while termination criterion is not fulfilled do
6    if gen ≥ 0.5 * MaxGen and rand > P then
7      MPool_1 ← TournamentSel (ArcCD);
8      Offspring_1 ← OperatorGA (MPool_1);
9      MPool_2 ← TournamentSel (Fitness);
10     Offspring_2 ← OperatorDE (MPool_2);
11   else
12     MPool_1 ← TournamentSel (PopCD);
13     Offspring_1 ← OperatorGA (MPool_1);
14     MPool_2 ← TournamentSel (Fitness);
15     Offspring_2 ← OperatorDE (MPool_2);
16   end if
17   Offspring ← (Offspring_1, Offspring_2)
18   UnionPop ← (Offspring, Pop)
19 end while
```

As shown in Fig. 5 is the main process of dual offspring generation strategy. The dual offspring strategy combines genetic algorithm and differential evolution to enhance exploration, development capabilities, improve population diversity, improve algorithm robustness through competitive selection and dynamic adjustment of search strategies.

III. EXPERIMENTAL SETUP

A. Experimental Setting

The experimental design used to evaluate the performance of the proposed HREA-AWC algorithm is introduced in detail. The experiment includes a series of benchmark problems, which are designed to comprehensively examine the performance of the algorithm in a multimodal multiobjective optimization environment. In addition, in order to quantify the performance of the algorithm, the study use multiple performance indicators, including key factors such as convergence and diversity of solutions. These indicators help us analyze and evaluate the effectiveness of the algorithm from different perspectives. Furthermore, in order to ensure the reliability and fairness of the experimental results, the paper also compare the HREA-AWC algorithm with several other advanced comparison algorithms. Through these comparative experiments, the advantages and potential improvement space of the HREA-AWC algorithm in dealing with complex optimization problems can be more clearly demonstrated.

1) Benchmark Problems: We used benchmark problems to verify the effectiveness of HREA-AWC in solving M-MOPs. Yue et al. [18] proposed multimodal multi-objective test functions (MMF). The MMF test problems consist of 19 test problems designed to evaluate the algorithm's ability and maintain multiple local Pareto optimal solutions. Liu et al. [16] proposed the imbalanced distance minimization problems (IDMP) with different search difficulties for different

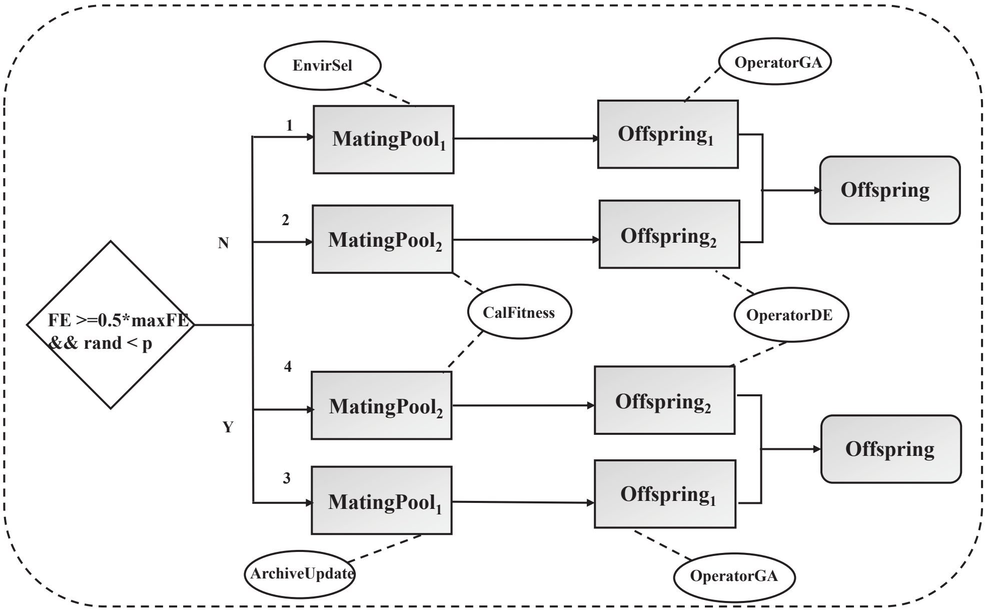

Fig. 5: A dual offspring generation.

PSs. IDMP is derived from distance minimization problems [19] and polygon-based problems [20]. The IDMP test problems include 12 test problems that assess the algorithm's performance in identifying and balancing multiple Pareto optima across different levels of difficulty. Additionally, it contains 3 test questions, which is HYL [21].

2) Performance Metrics: Traditional performance evaluation metrics, such as GD [22], IGD [23], and HV [24], are mainly used to evaluate the aggregation degree and distribution breadth of populations in the target space. However, for multimodal multiobjective problems (MMOPs), performance evaluation only in the target space is not enough, and the characteristics in the decision space also need to be considered. Therefore, the evaluation method should be extended from the target space to the decision space to comprehensively measure the performance of the algorithm. In this study used two widely adopted metrics IGDX [25] [26] and PSP [27] to comprehensively evaluate the performance of HREA-AWC in both the decision space and objective space.

IGDX measures the convergence and diversity of the obtained solutions in the decision space. The calculation method for IGDX performance indicators is as follows:

$$IGDX(B) = \frac{1}{|B^*|}\left(\sum_{y\in B^*}\min_{x\in B}\{ED(x,y)\}\right) \tag{5}$$

where B represents the non-dominated solutions in the entire population, while B^* denotes the true Pareto optimal solution set. $ED(x,y)$ represents the Euclidean distance between x and y. A smaller IGDX value is better, indicating that the non-dominated solutions in the population are closer to the true PF. This suggests that the non-dominated solutions can more accurately approach the true PF, thereby improving the performance of the optimization algorithm and the quality of the solutions.

PSP assesses the diversity of the solution set and its proximity to the true Pareto front. PSP is the result of CR divided by IGDX, where CR stands for cover rate. The calculation method for PSP performance indicators is as follows:

$$PSP(B) = \frac{CR(B)}{IGDX(B)} \tag{6}$$

The formula for calculating CR is as follows:

$$CR(B) = \left(\prod_{i=1}^{N}\delta_i\right)^{\frac{1}{2N}} \tag{7}$$

N represents the dimensionality of the objective space, and δ_i the formula is as follows:

$$\delta_i = \left(\frac{\min(x_i^{*,\max}, x_i^{\max}) - \max(x_i^{*,\min}, x_i^{\min})}{x_i^{*,\max} - x_i^{*,\min}}\right)^2 \tag{8}$$

where $x_i^{*,\min}$ and $x_i^{*,\max}$ are the minimum and maximum in the PSs. If $x_i^{*,\min}$ = $x_i^{*,\max}$, δ_i is considered as δ_i = 1. If $x_i^{\min} \geq x_i^{*,\max}$ or $x_i^{\max} \leq x_i^{*,\min}$, δ_i is set as 0.

3) Competitor Algorithms: To verify the effectiveness of HREA in solving MMOPs, this paper compares HREA-AWC with four state-of-the-art algorithms. These include TriMOEATAR [28], DNNSGAII [29], MO_Ring_PSO_SCD [30] and HREA [13]. The parameter settings of all the comparison algorithms are shown in Table I. Throughout the entire experimental process, the population size is set to 100, and the maximum number of iterations is set to 100,000. The specific parameter for each algorithm are set according to the original papers. All experiments are conducted using PlatEMO [31] v4.7 on a PC with an AMD Ryzen 5 4600U processor with Radeon Graphics and 512MB of memory.

IV. Results and Discussion

This section mainly analyzes the experimental results on different indicators. IGDX measures the convergence and diversity of the obtained solutions in the decision space. PSP assesses the diversity of the solution set and its proximity to the true Pareto front. In addition, we discussed the various components and parameters of HREA-AWC. Subsequently, in order to obtain comprehensive statistical conclusions, the

TABLE I: The parameter settings of the comparison algorithms

Algorithm	Parameters
TriMOEATAR	p_{con} = 0.5, σ_{niche} = 0.1, ε_{peak} =0.01
DNNSGAII	-
MO_Ring_PSO_SCD	C_1 = C_2 = 2.05, W = 0.7298, n_{PBA} = 5, n_{NBA} = 15, subsize=5, n_{GBA} = 10 * subsize
HREA	p = 0.5, ϵ = 0.3
HREA-AWC	p = 0.5, ϵ = 0.3, M = 10

wilcoxon rank sum test [32] was used to compare the results of HREA-AWC and other algorithms at a significance level of 0.05. The symbols ”+”, ”-”, and ”≈” indicate that the comparison algorithm is significantly better, significantly worse, or statistically equivalent to HREA-AWC. The average values and variances of IGDX and PSP over 30 runs are presented, with the best solutions are marked in bold.

A. Results on Benchmark

Table II shows the IGDX comparison results from which we can observe that HREA-AWC shows better performance than other state-of-the-art algorithms on the chosen test problems. Specifically, HREA-AWC wins 13 instances over 22 test problems. From the table, HREA-AWC, HREA and TriMOEATAR are shown to be the best two algorithms for solving the chosen problems. Notably, the DNNSGAII and MO_Ring_PSO_SCD did not show significant advantages on all test problems, and their IGDX values were generally high, indicating their limitations in solving complex multimodal multiobjective optimization problems. In summary, HREA-AWC is the most competitive algorithm in this experiment, demonstrating excellent performance on most test problems.

We also compare the PSP results for these algorithms in Table III, from which we can find that HREA-AWC, HREA, TriMOEATAR and DNNSGAII perform better than other algorithms. Specifically, HREA-AWC wins 15 instances over 22 test problems. From the table, the HREA-AWC exhibits significant advantages in most test problems. Compared with other algorithms, HREA-AWC significantly outperforms TriMOEATAR on 20 test problems, surpasses DNNSGAII on 19 test problems, and outperforms MO_Ring_PSO_SCD on all 22 test problems. Especially in the MMF, such as MMF1-MMF7 and MMF11-MMF15, their PSP values are the highest, and most of the results have statistical significance. Compared with the HREA, HREA-AWC performs equally well on 17 test problems. Although TriMOEATAR and DNNSGAII perform better in the MMF9 and MMF14_a, the proportion of such cases is extremely low. HREA-AWC is more stable in balancing diversity and convergence.

Table IV lists the IGDX results obtained by all the competitor algorithms. As we can see from the table, HREA-AWC wins 8 instances over 12 test problems. Compared to HREA, HREA shows a slightly better performance on IDMPM2T2. At the same time, on the IDMPM4T2 to IDMPM4T4 test problems, HREA-AWC is slightly inferior to MO_Ring_PSO_SCD. This is because the proposed HREA-AWC algorithm performs poorly in measuring the distribution and diversity of the solution set when facing complex objective functions and constraints.

In table V lists the PSP results obtained by all the competitor algorithms. HREA-AWC performs better than the other four algorithms on 9 test problems, while its performance is not satisfactory on the three test problems IDMPM4T2, IDMPM4T3, and IDMPM4T4. To summarize, HREA-AWC shows excellent ability in solving multimodal multiobjective optimization problem.

As shown in Fig. 6 and Fig. 7. By comparing the IGDX and PSP convergence curves of HREA-AWC and other algorithms on MMF6, HYL5, IDMPM3T2 and IDMPM4T1 test problems. From Fig. 6, it can be seen that the IGDX values of HREA-AWC and HREA are the smallest, while the IGDX values of the other three algorithms are relatively large. The smaller the IGDX, the better the algorithm performance. From Fig. 7 (a), (b) and (d), it can be seen that the PSP values of HREA-AWC and HREA are overall the highest, while the PSP values of the other three algorithms are relatively small. The larger the PSP, the better the algorithm performance. Specifically, the MO_Ring_PSO_SCD in Fig. 7 (c) has the highest PSP value during the 19 calculations, but during the last calculation, PSP suddenly decreases. The PSP value of HREA-AWC is generally good. In brief, it can be seen that the HREA-AWC algorithm has a faster convergence speed, indicating its high optimization accuracy. At the same time, the convergence curve of HREA-AWC shows stability and robustness, and can maintain excellent performance in different testing problems. Therefore, HREA-AWC demonstrates higher efficiency and reliability in various problems, outperforming other algorithms.

As shown in Fig. 8 to Fig.12 shows the distribution of the obtained solutions in the objective and decision spaces. The PSs are shown in the subfigures in upper right. In the MMF5 test problem, compared with the other three algorithms, HREA-AWC and HREA can simultaneously cover multiple dispersed Pareto sets in the decision space and evenly distribute them in the objective space. This indicates that it can effectively handle multimodal characteristics and avoid falling into local optima. In the HYL test problem, HREA-AWC and HREA have a wide distribution of solutions in the objective space without significant clustering, and the solutions are mapped to different regions in the decision space. They can maintain the diversity of high-dimensional problems and avoid solution set degradation caused by dimensional disasters. The TriMOEATAR algorithm significantly aggregates in the decision space, indicating that complex structures or high-dimensional characteristics may lead to overlapping solution sets. On MMF5 and HYL test problems, the solutions generated by the HREA-AWC algorithm may be more uniform or concentrated, demonstrating its ability to better balance the needs of various dimensions when optimizing objectives. HREA-AWC avoids local optima better than other algorithms and can search for more globally meaningful solutions in the solution space.

TABLE II: IGDX results of the proposed algorithm and compared algorithms on MMF and HYL

Problem	TriMOEATAR	DNNSGAII	MO_Ring_PSO_SCD	HREA	HREA-AWC
MMF1	1.0410e-1 (2.87e-2) −	6.9660e-2 (2.84e-3) −	1.4431e-1 (2.57e-2) −	5.6135e-2 (1.85e-3) ≈	5.5821e-2 (1.55e-3)
MMF2	9.5242e-2 (7.07e-2) −	1.2510e-2 (3.07e-3) −	5.9282e-2 (4.84e-2) −	8.3425e-3 (2.88e-4) −	8.0601e-3 (2.27e-4)
MMF3	5.7532e-2 (4.52e-2) −	2.0633e-2 (6.80e-3) −	2.4991e-2 (5.28e-3) −	8.3014e-3 (3.20e-4) −	8.0937e-3 (2.44e-4)
MMF4	1.3400e-1 (1.01e-1) −	5.2429e-2 (9.57e-3) −	2.3681e-1 (7.49e-2) −	3.2349e-2 (1.14e-3) ≈	3.2269e-2 (1.14e-3)
MMF5	1.9221e-1 (5.74e-2) −	1.3021e-1 (7.63e-3) −	2.7977e-1 (4.96e-2) −	9.4380e-2 (2.34e-3) ≈	9.3455e-2 (1.95e-3)
MMF6	1.5938e-1 (3.03e-2) −	1.1243e-1 (6.47e-3) −	2.2466e-1 (3.38e-2) −	8.4422e-2 (2.37e-3) ≈	8.3764e-2 (2.22e-3)
MMF7	7.0674e-2 (1.50e-2) −	3.8585e-2 (2.47e-3) −	1.5610e-1 (3.23e-2) −	3.4742e-2 (3.35e-3) ≈	3.3402e-2 (1.71e-3)
MMF8	1.3682e+0 (6.61e-1) −	1.0642e-1 (1.45e-2) −	6.6490e-1 (2.14e-1) −	6.6450e-2 (3.13e-3) ≈	6.8614e-2 (6.00e-3)
MMF9	3.4484e-3 (1.54e-6) +	1.1424e-2 (1.51e-3) +	4.4853e-2 (1.80e-2) −	1.7497e-2 (1.24e-3) ≈	1.7221e-2 (1.29e-3)
MMF10	8.0001e-1 (4.76e-7) −	6.5477e-1 (2.09e-1) −	7.9993e-1 (3.95e-4) −	2.4169e-1 (9.57e-2) ≈	2.2521e-1 (9.48e-2)
MMF11	7.5119e-1 (6.76e-8) −	7.4520e-1 (2.54e-3) −	7.4366e-1 (2.77e-3) −	6.8581e-2 (8.45e-2) ≈	4.9330e-2 (5.51e-2)
MMF12	7.7304e-1 (6.28e-6) −	7.6943e-1 (2.20e-3) −	7.6566e-1 (3.79e-3) −	3.1094e-1 (3.03e-3) ≈	3.1165e-1 (3.06e-3)
MMF13	NaN (NaN)	NaN (NaN)	NaN (NaN)	NaN (NaN)	NaN (NaN)
MMF14	2.5503e-1 (2.81e-3) −	2.9928e-1 (5.03e-2) −	4.3186e-1 (1.59e-1) −	2.3672e-1 (5.82e-2) ≈	2.4505e-1 (5.05e-2)
MMF14_a	7.8662e-2 (6.52e-2) −	2.9470e-1 (8.41e-2) −	4.6153e-1 (1.22e-1) −	1.7328e-3 (6.64e-3) ≈	8.2597e-4 (3.36e-3)
MMF15	7.5539e-1 (7.17e-4) −	7.4268e-1 (2.55e-2) −	6.5118e-1 (1.89e-1) −	2.2898e-1 (6.44e-2) ≈	2.1773e-1 (7.57e-2)
MMF15_a	2.3142e-1 (1.62e-3) −	2.2729e-1 (6.53e-3) −	2.3483e-1 (7.75e-3) −	1.0154e-1 (4.09e-3) ≈	1.0155e-1 (4.16e-3)
MMF1_e	7.6852e-2 (8.66e-4) +	8.3218e-2 (1.27e-2) ≈	8.6668e-2 (1.07e-2) ≈	1.6295e-1 (1.50e-1) ≈	1.5508e-1 (1.37e-1)
MMF1_z	2.8929e-1 (4.36e-1) ≈	1.0290e-1 (3.81e-2) ≈	8.9761e-2 (2.27e-2) ≈	9.1857e-2 (2.15e-2) ≈	8.5549e-2 (1.23e-2)
HYL1	1.3123e+0 (6.23e-1) −	2.6179e-1 (3.43e-2) −	3.7757e-1 (2.77e-2) −	1.7363e-1 (1.02e-2) ≈	1.7718e-1 (1.05e-2)
HYL2	7.0842e-1 (6.15e-2) −	8.7262e-1 (1.04e-1) −	1.7017e+0 (4.16e-1) −	5.0339e-1 (4.92e-2) ≈	5.2339e-1 (5.84e-2)
HYL5	5.2759e+0 (4.28e+0) −	2.9927e-1 (2.19e-2) −	4.5047e-1 (5.77e-2) −	2.4573e-1 (4.40e-3) ≈	2.4399e-1 (3.90e-3)
+ / − / ≈	2/18/1	1/18/2	0/19/2	0/2/19	

TABLE III: PSP results of the proposed algorithm and compared algorithms on MMF and HYL

Problem	TriMOEATAR	DNNSGAII	MO_Ring_PSO_SCD	HREA	HREA-AWC
MMF1	9.9665e+0 (2.36e+0) −	1.4377e+1 (5.92e-1) −	6.6745e+0 (1.25e+0) −	1.7813e+1 (5.59e-1) ≈	1.7915e+1 (4.83e-1)
MMF2	1.6519e+1 (1.24e+1) −	8.2147e+1 (1.11e+1) −	2.4720e+1 (1.49e+1) −	1.2001e+2 (4.11e+0) −	1.2416e+2 (3.48e+0)
MMF3	2.3727e+1 (1.43e+1) −	5.2181e+1 (1.27e+1) −	4.0948e+1 (8.82e+0) −	1.2062e+2 (4.38e+0) −	1.2366e+2 (3.67e+0)
MMF4	9.3473e+0 (3.48e+0) −	1.9570e+1 (2.88e+0) −	3.9668e+0 (1.64e+0) −	3.0940e+1 (1.08e+0) ≈	3.1023e+1 (1.12e+0)
MMF5	5.3432e+0 (1.23e+0) −	7.7006e+0 (4.36e-1) −	3.2945e+0 (7.14e-1) −	1.0592e+1 (2.60e-1) ≈	1.0697e+1 (2.23e-1)
MMF6	6.2460e+0 (1.37e+0) −	8.9202e+0 (5.03e-1) −	4.0837e+0 (8.81e-1) −	1.1848e+1 (3.31e-1) ≈	1.1933e+1 (3.12e-1)
MMF7	1.3580e+1 (4.04e+0) −	2.5969e+1 (1.64e+0) −	5.3712e+0 (1.64e+0) −	2.8964e+1 (2.48e+0) ≈	2.9970e+1 (1.48e+0)
MMF8	6.7707e-1 (4.45e-1) −	9.5426e+0 (1.31e+0) −	1.4218e+0 (5.03e-1) −	1.5041e+1 (7.23e-1) ≈	1.4577e+1 (1.17e+0)
MMF9	2.8999e+2 (1.30e-1) +	8.8799e+1 (9.99e+0) +	2.5269e+1 (8.65e+0) −	5.7408e+1 (3.78e+0) ≈	5.8379e+1 (4.31e+0)
MMF10	0.0000e+0 (0.00e+0) −	9.3501e-1 (1.14e+0) −	5.0096e+0 (1.62e+0) −	6.5583e+1 (6.53e+0) +	6.1725e+1 (6.59e+0)
MMF11	0.0000e+0 (0.00e+0) −	5.2909e-1 (4.47e-2) −	1.0313e+0 (5.23e-1) −	7.5033e+0 (5.91e-1) −	8.0523e+0 (4.20e-1)
MMF12	2.0424e-3 (1.05e-2) −	3.7396e-1 (3.50e-2) −	1.0769e+0 (5.52e-1) −	4.6710e+0 (4.80e-2) ≈	4.6902e+0 (4.52e-2)
MMF13	8.8109e-1 (6.72e-2) −	9.8503e-1 (7.93e-3) −	1.1295e+0 (1.98e-1) −	7.8391e+0 (1.58e+0) ≈	8.2142e+0 (1.73e+0)
MMF14	2.0623e+1 (3.74e-1) +	1.2158e+1 (1.77e+0) +	8.0277e+0 (1.12e+0) −	1.0978e+1 (7.05e-1) ≈	1.0964e+1 (9.90e-1)
MMF14_a	8.0987e+0 (8.84e-1) −	1.0787e+1 (1.03e+0) +	7.0368e+0 (1.21e+0) −	1.0200e+1 (8.30e-1) ≈	1.0201e+1 (7.41e-1)
MMF15	0.0000e+0 (0.00e+0) −	2.9904e+0 (3.40e-1) −	4.2890e+0 (4.40e-1) −	6.5131e+0 (4.10e-1) −	6.7642e+0 (3.72e-1)
MMF15_a	3.4282e+0 (3.07e-2) −	3.6441e+0 (2.23e-1) −	3.6869e+0 (3.15e-1) −	9.8629e+0 (3.98e-1) ≈	9.8634e+0 (4.04e-1)
MMF1_e	2.2032e+0 (4.98e-1) −	3.3242e+0 (5.62e-1) −	2.9944e+0 (3.71e-1) −	4.0705e+0 (4.30e-1) ≈	4.1021e+0 (4.68e-1)
MMF1_z	3.6168e+0 (1.12e+0) −	5.1785e+0 (1.17e-1) −	3.7987e+0 (5.71e-1) −	5.7303e+0 (1.22e-1) ≈	5.7706e+0 (7.68e-2)
HYL1	6.3961e-1 (3.41e-1) −	3.8772e+0 (4.64e-1) −	2.6488e+0 (1.90e-1) −	5.7780e+0 (3.29e-1) ≈	5.6631e+0 (3.37e-1)
HYL2	1.3779e+0 (1.27e-1) −	1.1619e+0 (1.39e-1) −	5.8986e-1 (1.51e-1) −	2.0044e+0 (1.90e-1) ≈	1.9323e+0 (2.03e-1)
HYL5	1.4503e+0 (1.99e+0) −	3.3521e+0 (2.25e-1) −	2.2536e+0 (2.76e-1) −	4.0661e+0 (7.47e-2) ≈	4.0944e+0 (6.83e-2)
+ / − / ≈	2/20/0	3/19/0	0/22/0	1/4/17	

TABLE IV: IGDX results of the proposed algorithm and compared algorithms on IDMP

Problem	TriMOEATAR	DNNSGAII	MO_Ring_PSO_SCD	HREA	HREA-AWC
IDMPM2T1	6.5183e-1 (1.17e-1) −	6.0616e-1 (2.05e-1) −	3.0356e-1 (3.29e-1) −	1.1773e-3 (1.67e-4) −	1.0578e-3 (1.16e-5)
IDMPM2T2	6.0735e-1 (2.01e-1) −	4.7190e-1 (3.13e-1) −	7.0020e-3 (5.11e-3) −	1.3860e-3 (1.14e-4) +	1.5440e-3 (7.37e-5)
IDMPM2T3	4.4234e-1 (3.11e-1) −	2.1181e-1 (3.08e-1) −	4.0461e-3 (1.09e-3) −	2.3737e-3 (5.49e-4) −	1.8240e-3 (9.26e-5)
IDMPM2T4	6.7328e-1 (2.97e-5) −	6.2858e-1 (1.71e-1) −	9.8821e-3 (8.00e-3) −	2.2685e-3 (3.87e-3) −	1.0580e-3 (9.54e-6)
IDMPM3T1	6.7305e-1 (2.63e-1) −	6.7845e-1 (2.86e-1) −	2.5309e-1 (2.08e-1) −	1.2379e-2 (3.20e-4) −	1.2217e-2 (2.22e-4)
IDMPM3T2	7.5858e-1 (2.41e-1) −	6.7157e-1 (2.38e-1) −	1.8264e-1 (1.73e-1) −	1.3115e-2 (2.11e-3) −	1.2226e-2 (2.62e-4)
IDMPM3T3	6.7903e-1 (2.41e-1) −	6.5217e-1 (3.10e-1) −	3.0620e-2 (4.46e-2) −	1.4852e-2 (3.29e-3) −	1.2682e-2 (3.19e-4)
IDMPM3T4	8.5772e-1 (2.41e-1) −	8.2122e-1 (2.51e-1) −	2.5462e-1 (2.01e-1) −	1.3582e-2 (2.66e-3) −	1.2169e-2 (2.33e-4)
IDMPM4T1	1.1631e+0 (1.12e-1) −	1.1168e+0 (1.63e-1) −	1.0106e+0 (2.68e-1) −	7.3251e-1 (3.71e-1) −	2.1040e-1 (2.09e-1)
IDMPM4T2	1.1195e+0 (1.21e-1) −	1.0598e+0 (1.68e-1) −	5.1494e-1 (2.74e-1) ≈	9.7951e-1 (3.14e-1) −	7.7024e-1 (2.97e-1)
IDMPM4T3	1.0883e+0 (1.39e-1) −	9.7604e-1 (1.88e-1) −	1.1480e-1 (1.18e-1) ≈	8.2107e-1 (3.18e-1) −	2.7634e-1 (2.24e-1)
IDMPM4T4	1.1000e+0 (1.07e-1) −	1.0927e+0 (1.25e-1) −	4.8810e-1 (3.00e-1) +	1.0634e+0 (2.09e-1) −	8.1183e-1 (3.01e-1)
+ / − / ≈	0/12/0	0/12/0	1/9/2	1/11/0	

TABLE V: PSP results of the proposed algorithm and compared algorithms on IDMP

Problem	TriMOEATAR	DNNSGAII	MO_Ring_PSO_SCD	HREA	HREA-AWC
IDMPM2T1	3.3805e-2 (1.67e-1) −	1.1610e-1 (3.27e-1) −	5.7296e-1 (4.90e-1) −	1.0787e+0 (3.46e-3) −	1.0809e+0 (1.73e-3)
IDMPM2T2	1.0898e-1 (3.10e-1) −	3.3681e-1 (4.95e-1) −	1.0509e+0 (4.02e-2) −	1.0817e+0 (1.14e-3) −	1.0824e+0 (1.01e-3)
IDMPM2T3	3.4772e-1 (4.48e-1) −	7.0408e-1 (4.58e-1) −	1.0324e+0 (1.08e-2) −	1.0338e+0 (5.41e-3) −	1.0385e+0 (1.17e-3)
IDMPM2T4	3.5057e-3 (1.40e-3) −	7.9146e-2 (2.71e-1) −	1.0305e+0 (4.64e-2) −	1.0761e+0 (1.42e-2) −	1.0814e+0 (3.00e-4)
IDMPM3T1	3.3056e-1 (3.10e-1) −	4.0989e-1 (4.21e-1) −	8.7491e-1 (2.67e-1) −	1.2217e+0 (2.35e-2) ≈	1.2291e+0 (1.50e-2)
IDMPM3T2	2.5910e-1 (3.08e-1) −	3.8890e-1 (3.77e-1) −	1.0425e+0 (2.25e-1) −	1.2210e+0 (1.98e-2) ≈	1.2226e+0 (1.83e-2)
IDMPM3T3	3.8275e-1 (3.42e-1) −	4.0796e-1 (4.00e-1) −	1.1781e+0 (6.67e-2) ≈	1.1675e+0 (5.77e-2) −	1.2139e+0 (2.05e-2)
IDMPM3T4	1.3254e-1 (2.93e-1) −	2.4827e-1 (3.76e-1) −	8.8208e-1 (3.02e-1) −	1.2093e+0 (3.33e-2) ≈	1.2235e+0 (1.83e-2)
IDMPM4T1	2.0744e-2 (6.08e-2) −	5.1101e-2 (8.84e-2) −	2.1301e-1 (3.36e-1) −	4.3918e-1 (4.09e-1) −	1.0227e+0 (2.69e-1)
IDMPM4T2	1.7803e-2 (4.73e-2) −	5.4188e-2 (8.75e-2) −	5.9016e-1 (3.26e-1) +	1.7909e-1 (3.08e-1) −	3.0531e-1 (3.30e-1)
IDMPM4T3	3.2687e-2 (4.88e-2) −	9.2892e-2 (1.15e-1) −	1.0789e+0 (1.64e-1) ≈	3.0855e-1 (3.44e-1) −	9.2408e-1 (3.30e-1)
IDMPM4T4	7.8151e-3 (3.87e-3) −	2.3724e-2 (4.55e-2) −	6.7954e-1 (3.76e-1) +	7.6139e-2 (1.45e-1) −	3.0504e-1 (3.67e-1)
+/ − / ≈	0/12/0	0/12/0	2/8/2	0/9/3	

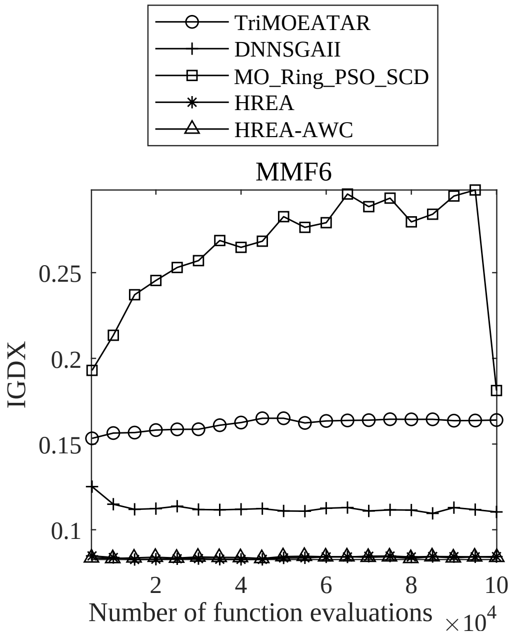

(a) MMF6

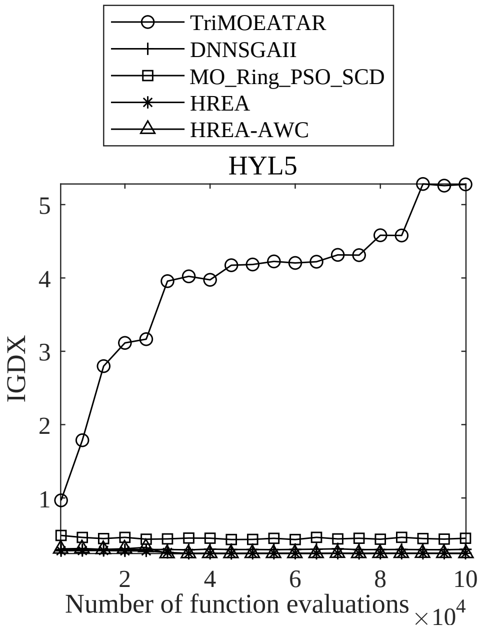

(b) HYL5

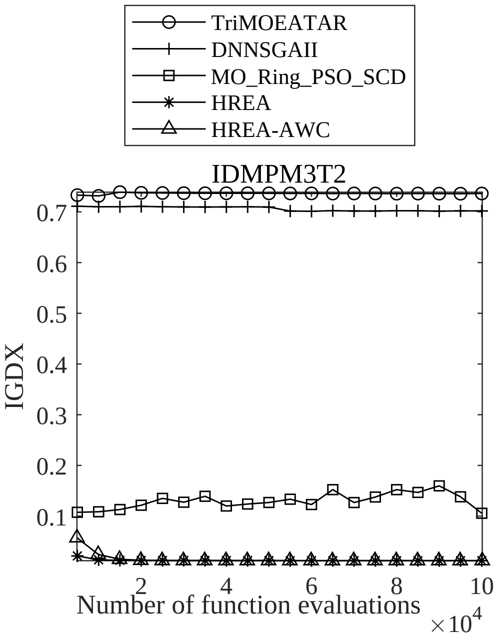

(c) IDMPM3T2

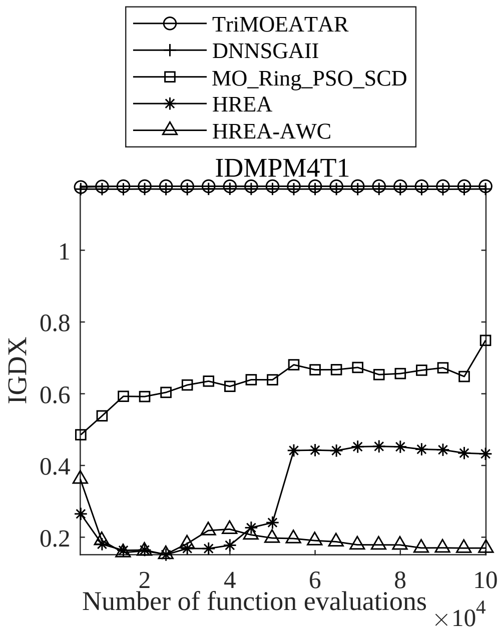

(d) IDMPM4T1

Fig. 6: The convergence profiles of IGDX obtained by the algorithms.

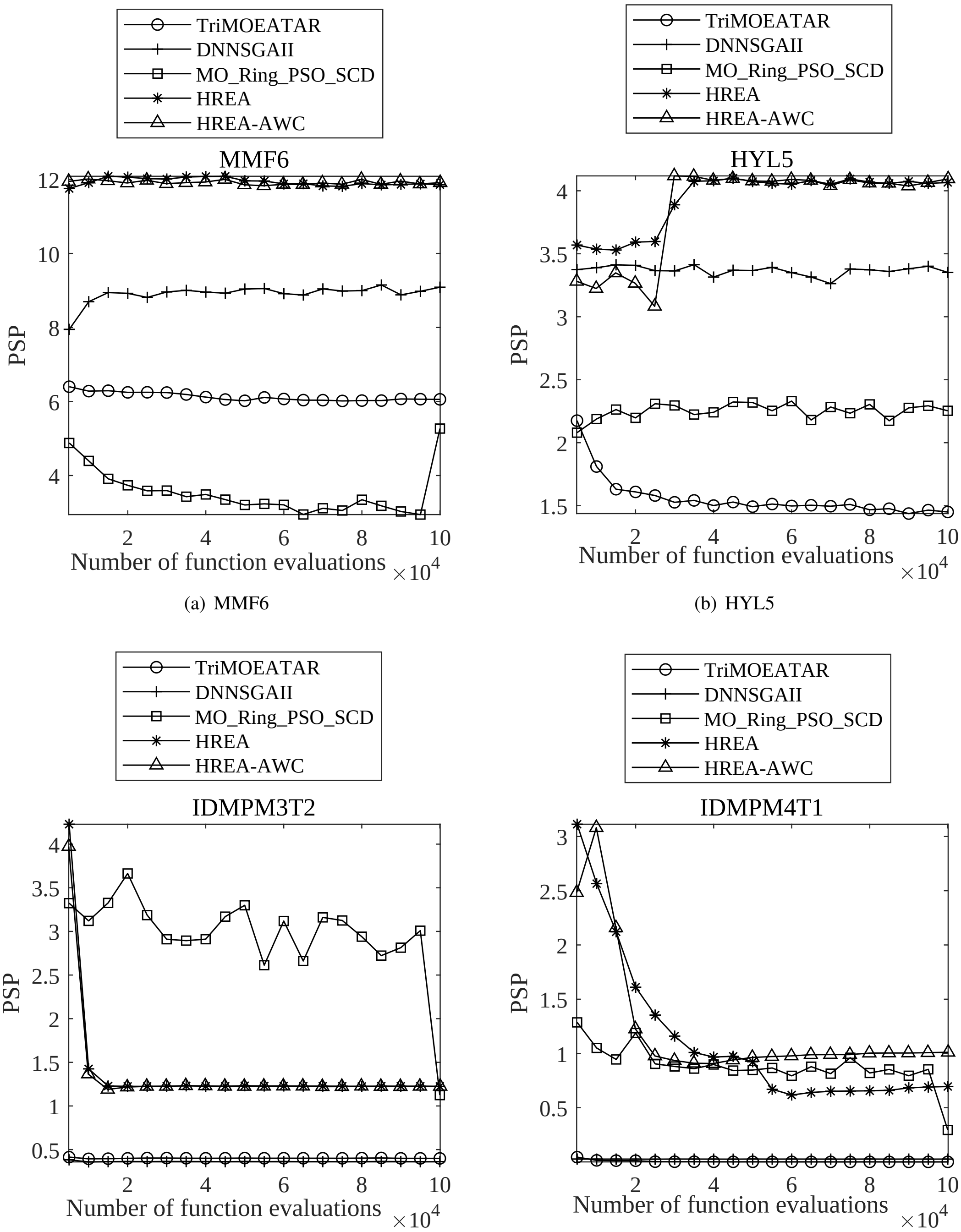

(a) MMF6 (b) HYL5

(c) IDMPM3T2 (d) IDMPM4T1

Fig. 7: The convergence profiles of PSP obtained by the algorithms.

As shown in Fig. 13 to Fig. 16. Objective space distribution under test problem MMF14_a when the number of evaluations reaches 25%, 50%, 75%, 100%. At the 25% stage, TriMOEATAR exhibits significant exploration ability in the objective space, with its solution set widely distributed in multiple potential regions of the Pareto front (PF). The solution set of MO_Ring_PSO_SCD is excessively concentrated on the left end of PF. HREA-AWC, HREA, and DNNSGAII, although their partial decomposition deviates from the true PF, cover more than half of the PF region in their distribution range. At the 50% stage and 75% stage, the solution sets of HREA-AWC and HREA gradually converge towards the true PF. In contrast, TriMOEATAR, MO_Ring_PSO_SCD, and DNNSGAII did not show significant changes compared to the 25% stage. At the 100% stage, the solution sets of HREA-AWC and HREA are widely distributed in multiple potential regions of the objective space. The performance indicators IGDX and PSP values of HREA-AWC are the best among them, indicating that HREA-AWC has a certain improvement in the accuracy of the solution.

V. Conclusion

This paper proposed an improved hierarchy ranking method with adaptive weighted coefficient for multimodal multiobjective optimization. During population production, offspring were generated using genetic and differential evolution strategies. In the environmental selection phase, adaptive

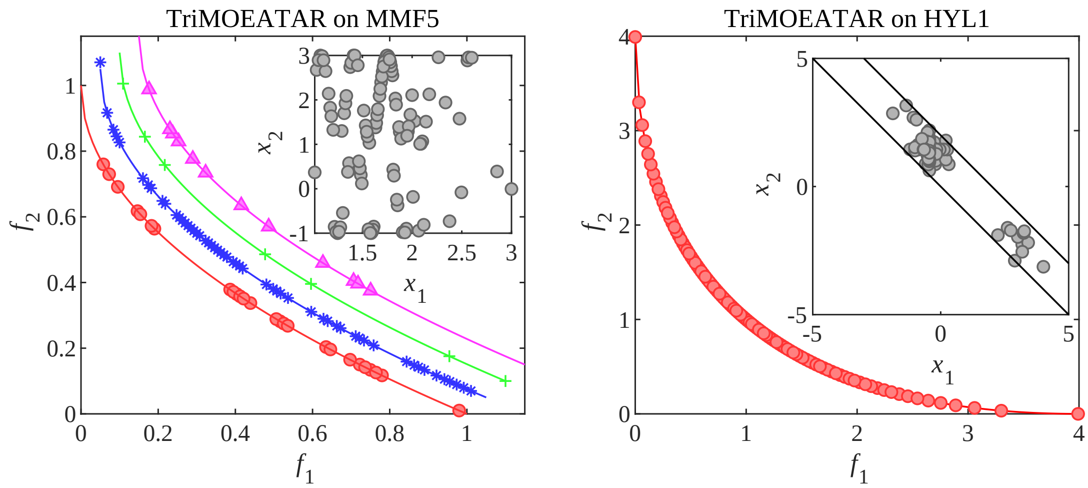

(a) MMF5 (b) HYL1

Fig. 8: Distribution of the obtained by TRiMOEATAR in the decision and objective space.

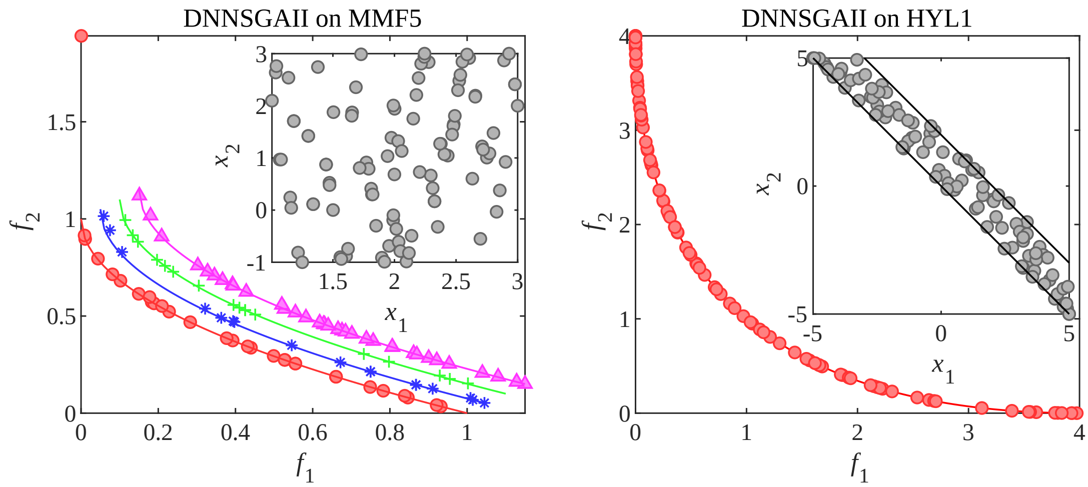

(a) MMF5 (b) HYL1

Fig. 9: Distribution of the obtained by DNNSGAII in the decision and objective space.

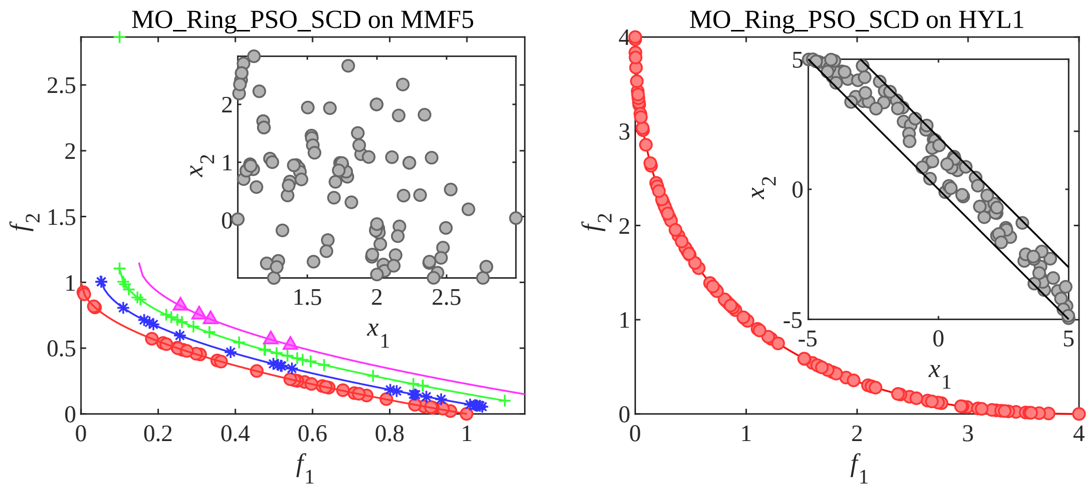

(a) MMF5 (b) HYL1

Fig. 10: Distribution of the obtained by MO_Ring_PSO_SCD in the decision and objective space.

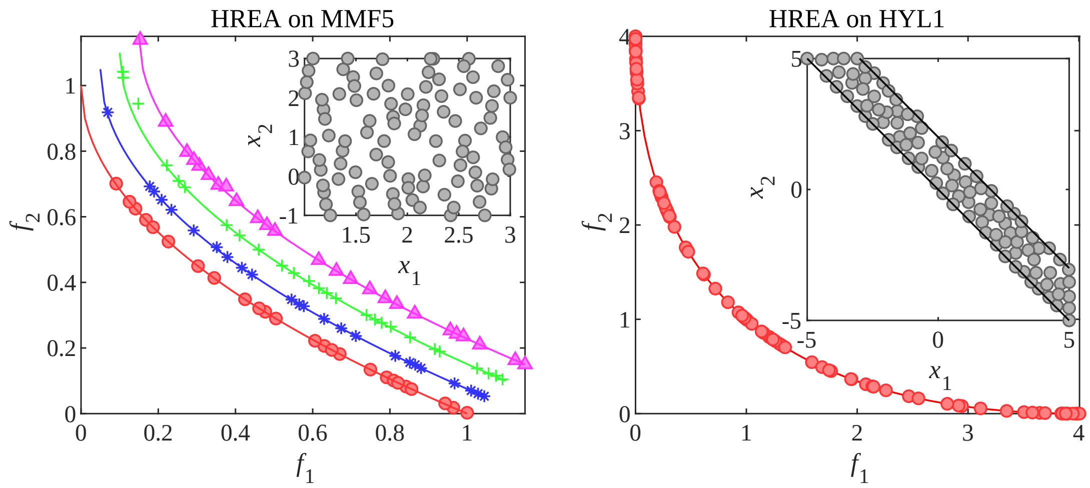

(a) MMF5 (b) HYL1

Fig. 11: Distribution of the obtained by HREA in the decision and objective space.

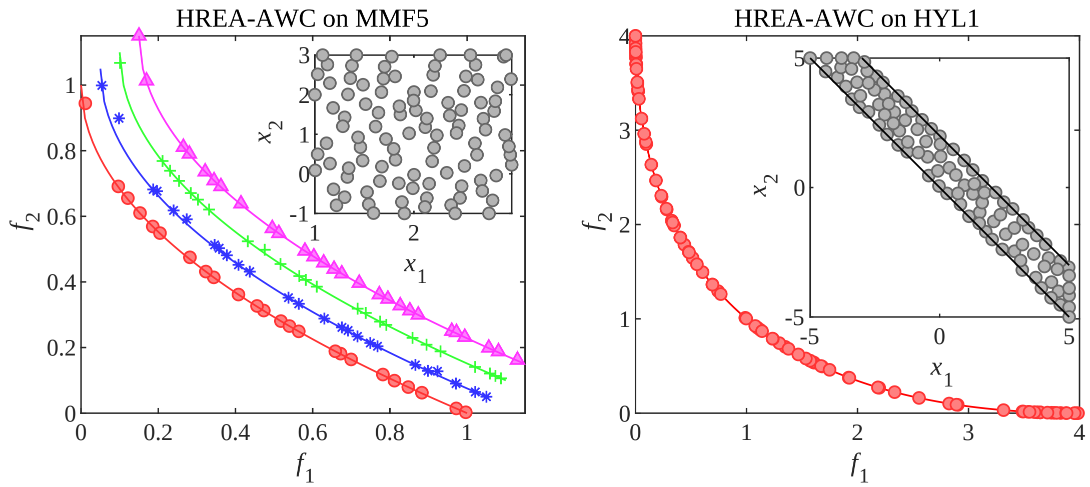

(a) MMF5 (b) HYL1

Fig. 12: Distribution of the obtained by HREA-AWC in the decision and objective space.

coefficients determine the priority of each individual, while the crowding distance between individuals was calculated using the 2-norm. On 34 test problems, this algorithm remains competitive compared to four other algorithms that are widely used. The proposed algorithm can more closely approach the true Pareto front and the convergence of the obtained non-dominated solutions. Although HREA-AWC has shown competitiveness, more work is still needed.In future, the HREA-AWC will be evaluated through additional test questions improving the distribution and diversity of the solution set.

References

[1] Y. H.J. Xuan, D.M. Zhou, "Constrained multi-objective optimization algorithm based on the boundary value reservation strategy," *IAENG International Journal of Applied Mathematics*, vol. 5, no. 2, pp. 297–306, 2025.

[2] R. Tanabe and H. Ishibuchi, "A review of evolutionary multimodal multiobjective optimization," *IEEE Transactions on Evolutionary Computation*, vol. 24, no. 1, pp. 193–200, 2020.

[3] S. Long, J. Zheng, Q. Deng, Y. Liu, J. Zou, and S. Yang, "A similarity-detection-based evolutionary algorithm for large-scale multimodal multi-objective optimization," *Swarm and Evolutionary Computation*, vol. 87, p. 101548, 2024.

[4] X. Yao, W. Li, X. Pan, and R. Wang, "Multimodal multi-objective evolutionary algorithm for multiple path planning," *Computers & Industrial Engineering*, vol. 169, p. 108145, 2022.

[5] J. Liu, X. Zhao, R. Ma, H. Xuan, X. Guo, and W. Zhai, "Multi-objective model and genetic algorithm for multisource multicast vnf service chain deployment problem." *IAENG International Journal of Computer Science*, vol. 51, no. 6, pp. 562–571, 2024.

[6] N. Li, L. Wang, L. Lin, and H. Xuan, "Multi-objective optimization model and improved genetic algorithm based on moea/d for vnf-sc deployment." *IAENG International Journal of Computer Science*, vol. 50, no. 1, pp. 172–181, 2023.

[7] G. Lapizco-Encinas, C. Kingsford, and J. Reggia, "Particle swarm optimization for multimodal combinatorial problems and its application to protein design," in *IEEE Congress on Evolutionary Computation*, 2010, pp. 1–8.

[8] K. Deb, A. Pratap, S. Agarwal, and T. Meyarivan, "A fast and elitist multiobjective genetic algorithm: Nsga-ii," *IEEE Transactions on Evolutionary Computation*, vol. 6, no. 2, pp. 182–197, 2002.

[9] Q. Zhang and H. Li, "Moea/d: A multiobjective evolutionary algorithm based on decomposition," *IEEE Transactions on Evolutionary Computation*, vol. 11, no. 6, pp. 712–731, 2007.

[10] H. Xuan, S. Wei, X. Zhao, Y. Zhou, D. Liu, and Y. Li, "Unavailable time aware scheduling of hybrid task on heterogeneous distributed system," *IAENG International Journal of Applied Mathematics*, vol. 50, no. 1, pp. 133–146, 2020.

[11] X. Ru, "An improved butterfly optimization algorithm for numerical optimization and parameter identification of photovoltaic model." *Engineering Letters*, vol. 33, no. 1, pp. 169–184, 2025.

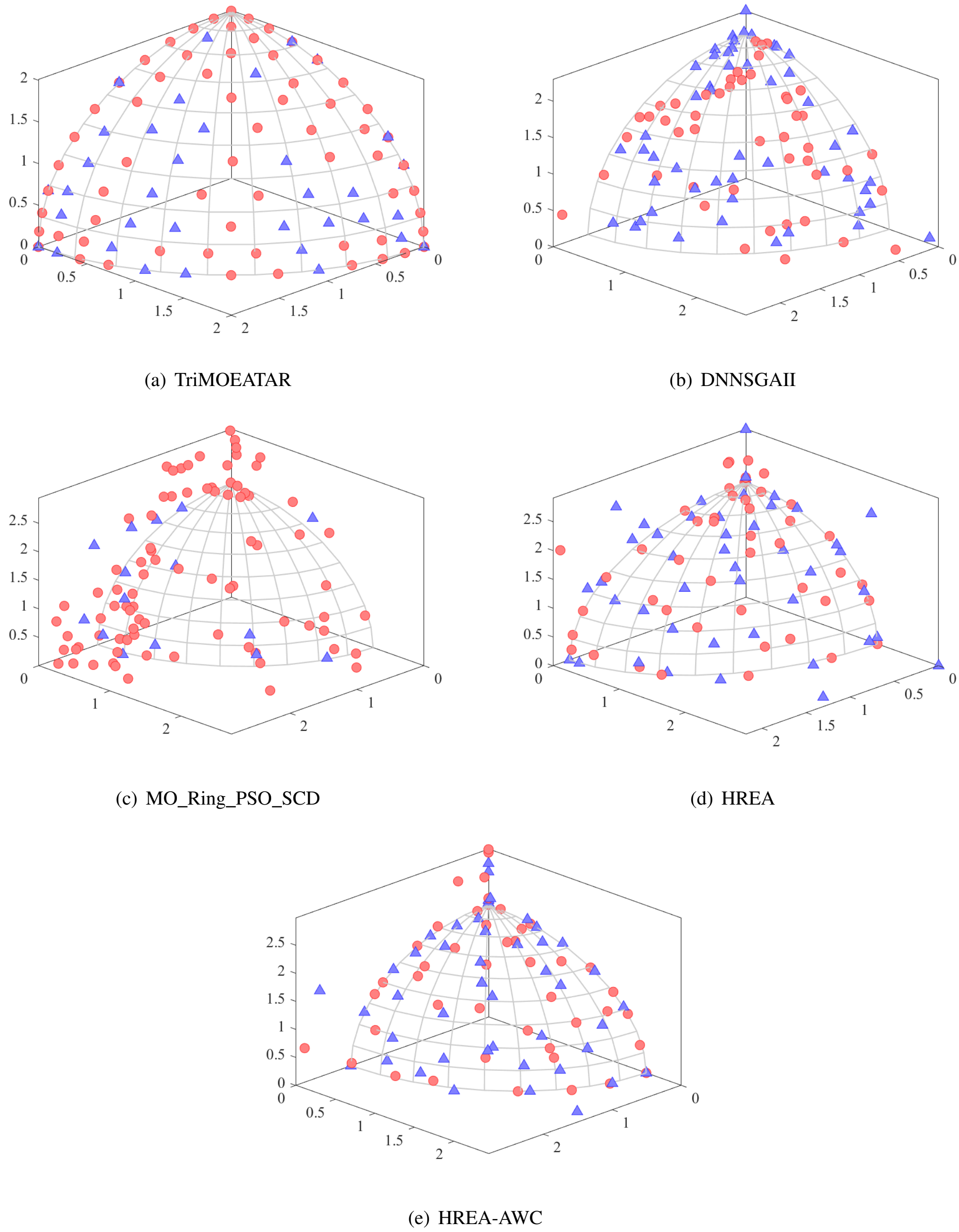

(a) TriMOEATAR (b) DNNSGAII

(c) MO_Ring_PSO_SCD (d) HREA

(e) HREA-AWC

Fig. 13: Objective space distribution on MMF14_a when the number of evaluations reaches to 25%.

[12] R. Wang, R. C. Purshouse, and P. J. Fleming, "Preference-inspired coevolutionary algorithms for many-objective optimization," *IEEE Transactions on Evolutionary Computation*, vol. 17, no. 4, pp. 474–494, 2012.

[13] W. Li, X. Yao, T. Zhang, R. Wang, and L. Wang, "Hierarchy ranking method for multimodal multiobjective optimization with local pareto fronts," *IEEE Transactions on Evolutionary Computation*, vol. 27, no. 1, pp. 98–110, 2023.

[14] Y. Tian, T. Zhang, J. Xiao, X. Zhang, and Y. Jin, "A coevolutionary framework for constrained multiobjective optimization problems," *IEEE Transactions on Evolutionary Computation*, vol. 25, no. 1, pp. 102–116, 2021.

[15] M. Ming, A. Trivedi, R. Wang, D. Srinivasan, and T. Zhang, "A dual-population-based evolutionary algorithm for constrained multiobjective optimization," *IEEE Transactions on Evolutionary Computation*, vol. 25, no. 4, pp. 739–753, 2021.

[16] Y. Liu, H. Ishibuchi, G. G. Yen, Y. Nojima, and N. Masuyama, "Handling imbalance between convergence and diversity in the decision space in evolutionary multimodal multiobjective optimization," *IEEE Transactions on Evolutionary Computation*, vol. 24, no. 3, pp. 551–565, 2020.

[17] W. Li, T. Zhang, R. Wang, and H. Ishibuchi, "Weighted indicator-based evolutionary algorithm for multimodal multiobjective optimization," *IEEE Transactions on Evolutionary Computation*, vol. 25, no. 6, pp. 1064–1078, 2021.

[18] C. Yue, B. Qu, K. Yu, J. Liang, and X. Li, "A novel scalable test problem suite for multimodal multiobjective optimization," *Swarm and Evolutionary Computation*, vol. 48, pp. 62–71, 2019.

[19] M. Köppen and K. Yoshida, "Substitute distance assignments in nsga-ii for handling many-objective optimization problems," in *Evolutionary Multi-Criterion Optimization*. Springer Berlin Heidelberg, 2007, pp. 727–741.

[20] H. Ishibuchi, Y. Hitotsuyanagi, N. Tsukamoto, and Y. Nojima, "Many-objective test problems to visually examine the behavior of multiobjective evolution in a decision space," in *Parallel Problem Solving from Nature, PPSN XI*. Springer Berlin Heidelberg, 2010, pp. 91–100.

[21] H. Ishibuchi, Y. Peng, and L. M. Pang, "Multi-modal multi-objective test problems with an infinite number of equivalent pareto sets," in *2022 IEEE congress on evolutionary computation (CEC)*. IEEE, 2022, pp. 1–8.

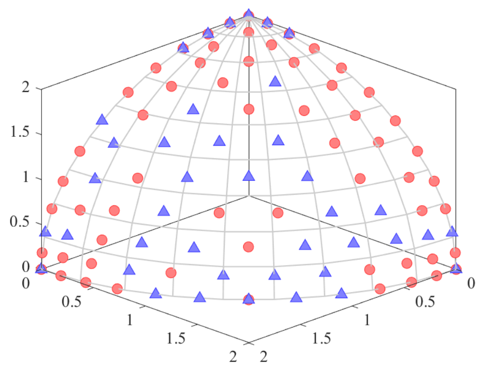

(a) TriMOEATAR

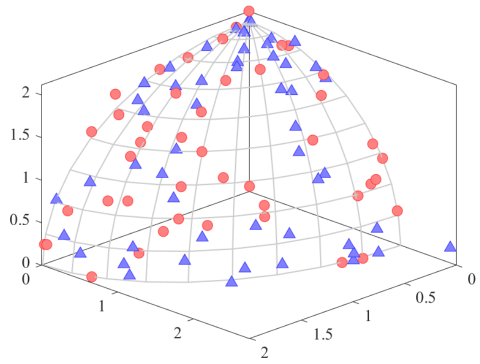

(b) DNNSGAII

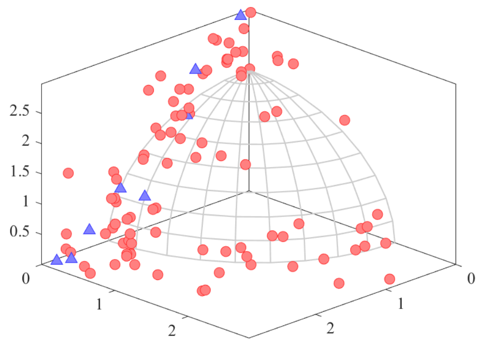

(c) MO_Ring_PSO_SCD

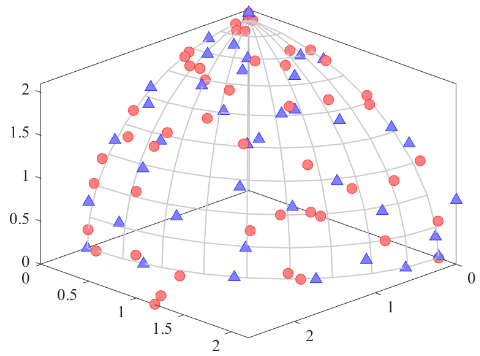

(d) HREA

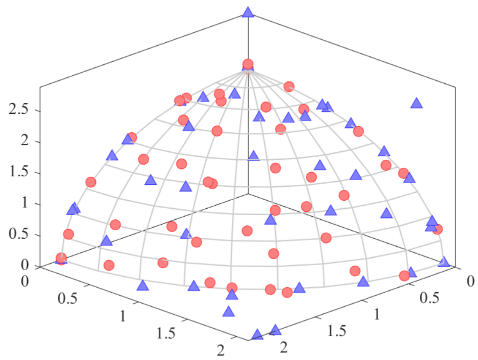

(e) HREA-AWC

Fig. 14: Objective space distribution on MMF14_a when the number of evaluations reaches to 50%.

[22] D. Van Veldhuizen and G. Lamont, "On measuring multiobjective evolutionary algorithm performance," in *Proceedings of the 2000 Congress on Evolutionary Computation*, vol. 1, 2000, pp. 204–211.

[23] P. A. Bosman and D. Thierens, "The balance between proximity and diversity in multiobjective evolutionary algorithms," *IEEE transactions on evolutionary computation*, vol. 7, no. 2, pp. 174–188, 2003.

[24] J. Bader and E. Zitzler, "Hype: An algorithm for fast hypervolume-based many-objective optimization," *Evolutionary Computation*, vol. 19, no. 1, pp. 45–76, 2011.

[25] A. Zhou, Q. Zhang, and Y. Jin, "Approximating the set of pareto-optimal solutions in both the decision and objective spaces by an estimation of distribution algorithm," *IEEE Transactions on Evolutionary Computation*, vol. 13, no. 5, pp. 1167–1189, 2009.

[26] R. Tanabe and H. Ishibuchi, "A niching indicator-based multi-modal many-objective optimizer," *Swarm and Evolutionary Computation*, vol. 49, pp. 134–146, 2019.

[27] C. Yue, B. Qu, and J. Liang, "A multiobjective particle swarm optimizer using ring topology for solving multimodal multiobjective problems," *IEEE Transactions on Evolutionary Computation*, vol. 22, no. 5, pp. 805–817, 2018.

[28] Y. Liu, G. G. Yen, and D. Gong, "A multimodal multiobjective evolutionary algorithm using two-archive and recombination strategies," *IEEE Transactions on Evolutionary Computation*, vol. 23, no. 4, pp. 660–674, 2019.

[29] J. J. Liang, C. T. Yue, and B. Y. Qu, "Multimodal multi-objective optimization: A preliminary study," in *2016 IEEE Congress on Evolutionary Computation (CEC)*, 2016, pp. 2454–2461.

[30] C. Yue, B. Qu, and J. Liang, "A multiobjective particle swarm optimizer using ring topology for solving multimodal multiobjective problems," *IEEE Transactions on Evolutionary Computation*, vol. 22, no. 5, pp. 805–817, 2018.

[31] Y. Tian, R. Cheng, X. Zhang, and Y. Jin, "Platemo: A matlab platform for evolutionary multi-objective optimization [educational forum]," *IEEE Computational Intelligence Magazine*, vol. 12, no. 4, pp. 73–87, 2017.

[32] J. Derrac, S. Garcła, D. Molina, and F. Herrera, "A practical tutorial on the use of nonparametric statistical tests as a methodology for comparing evolutionary and swarm intelligence algorithms," *Swarm and Evolutionary Computation*, vol. 1, no. 1, pp. 3–18, 2011.

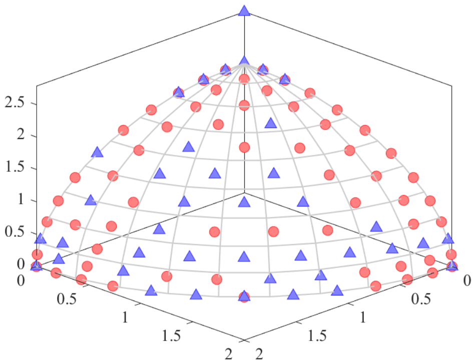

(a) TriMOEATAR

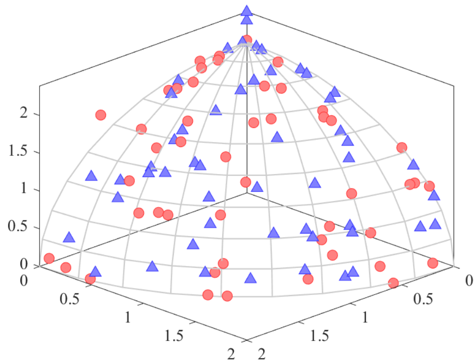

(b) DNNSGAII

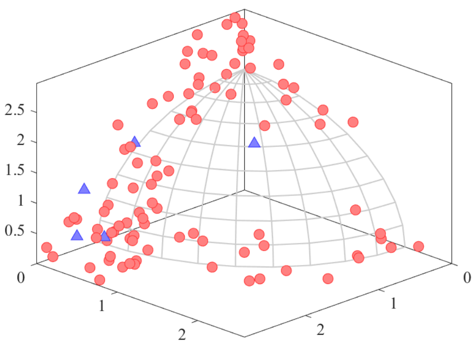

(c) MO_Ring_PSO_SCD

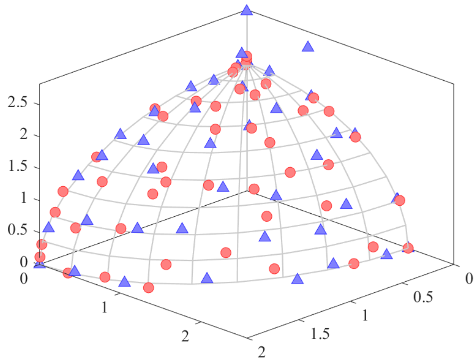

(d) HREA

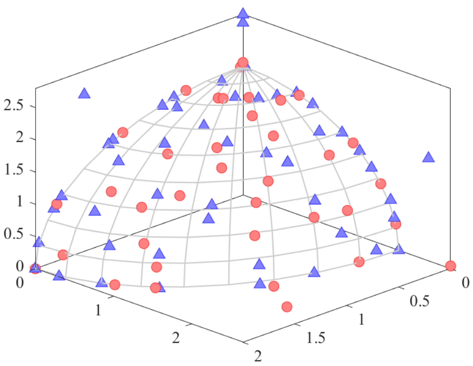

(e) HREA-AWC

Fig. 15: Objective space distribution on MMF14_a when the number of evaluations reaches to 75%.

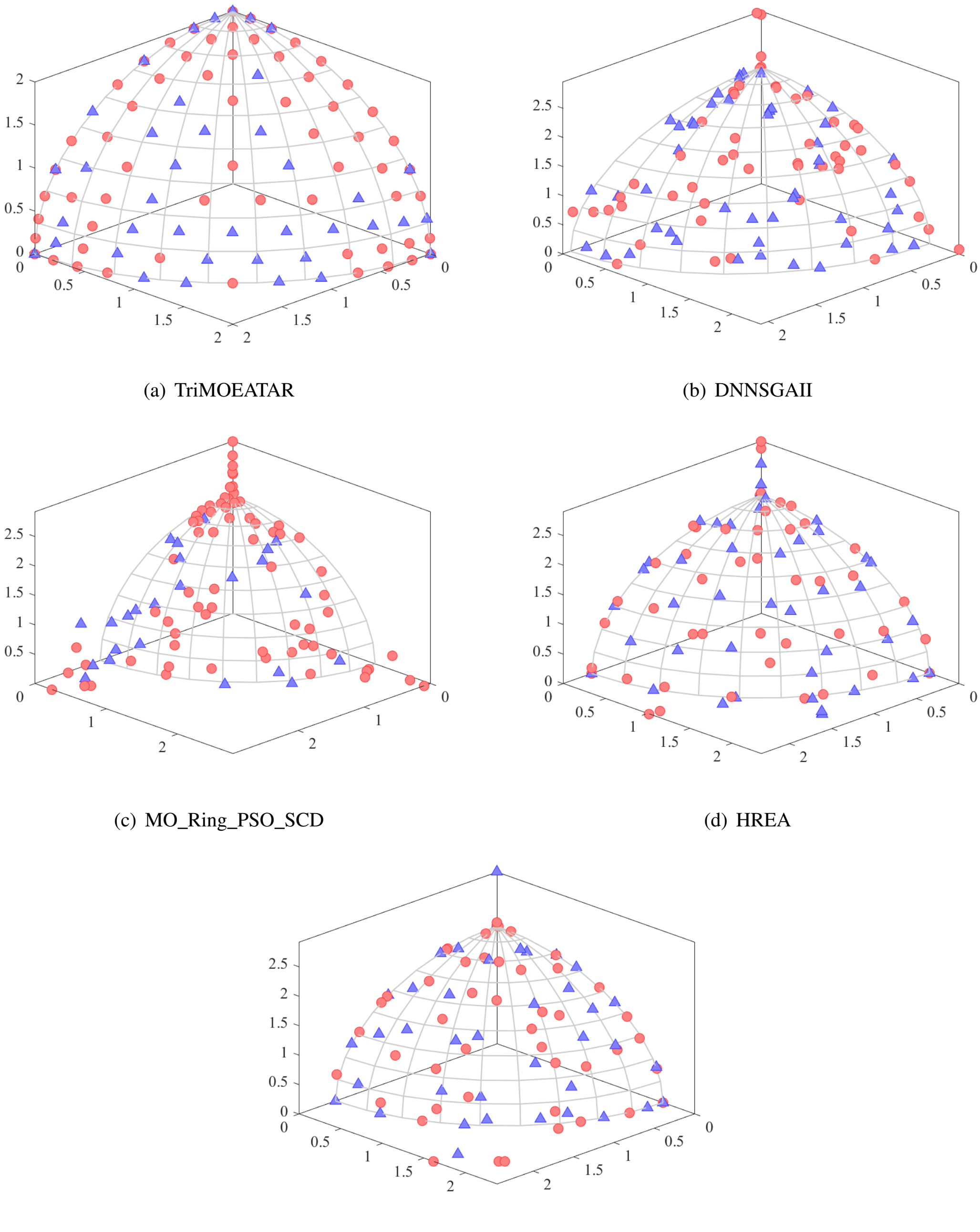

(a) TriMOEATAR

(b) DNNSGAII

(c) MO_Ring_PSO_SCD

(d) HREA

(e) HREA-AWC

Fig. 16: Objective space distribution on MMF14_a when the number of evaluations reaches to 100%.